



Phytoplankton, pelagic community and nutrients in a deep oligotrophic alpine lake: ratios as sensitive indicators of the use of P-resources (DRP:DOP:PP and TN:TP:SRSi)

Katrin Teubner*

Institute of Limnology, Austrian Academy of Sciences, Mondseestrasse 9, A-5310 Mondsee, Austria

Received 25 February 2002; received in revised form 4 September 2002; accepted 4 November 2002

Abstract

The different use of P-resources between two sites in the deep oligotrophic Traunsee was studied by seasonal and vertical patterns of phytoplankton and nutrients from 12/1997 to 10/1998. The P-resources were evaluated from the proportion between the P-fractions, the dissolved reactive P (DRP), dissolved non-reactive P (DOP) and particulate organic P (PP) and from the stoichiometry between nutrients, the total N (TN), the total P (TP) and soluble reactive Si (SRSi). Significant differences between an inshore site impacted by industrial tailings (Ebensee Bay, EB) and an open water reference site (Viechtau, VI) were evident from vertical profiles of both the P-accumulation (%PP of TP) evaluated by DRP:DOP:PP and the distribution of phytoplankton assessed by Si-exhaustion (TN:TP:SRSi), but not from the seasonal patterns of phytoplankton composition, S:V ratios of the algal community or surface layer nutrient dynamics. Low TP and the stable stratification from May to September triggered the relative accumulation of epilimnetic P at VI as it was evident from both the higher portion of particulate P within TP (%PP of TP) and from the shift towards P-enrichment in nutrient stoichiometry of TN:TP:SRSi. The predominance of around 55–52% algal carbon over bacteria at the surface layer to 20 m coincided spatially with the lowest Si content relative to N and P. The disturbances at the impacted site was summarised by: up to 11% less P accumulation by organisms at the surface, no stoichiometric shift towards TP in the epilimnion when compared with deeper layers and a reduction of the trophogenic zone to the top 10 m. Reasons for this disturbance are seen in the unstable stratification, turbidity, higher TP and the metazoan dominated food chain. Both triple ratios, DRP:DOP:PP and TN:TP:SRSi, were sensitive indicators of the use of P-resources by plankton communities, while inorganic dissolved fractions (DIN:DRP:SRSi, DIN = dissolved inorganic N) provided only insufficient information on nutrient resources in Traunsee.

© 2002 Elsevier Science Ltd. All rights reserved.

Keywords: Silica; Nitrogen; Phosphorus; Algae; Limitation; Fractions

1. Introduction

A number of recent limnological discoveries emphasise changes in plankton assemblages on both spatial and temporal scales. The vertical distribution of phytoplankton in the euphotic zone and even in deeper

layers is not constant in time or space as highlighted by studies on, e.g. the deep chlorophyll maximum and the vertical migration of algae. Light climate, mixing events, grazing, nutrient concentrations and their availability relative to other elements can be of decisive importance for the distribution pattern of algae in the water column. The seasonality of community structure is evidenced by changes in species composition and size spectra of algae (e.g. [1]) controlled simultaneously or alternatively from bottom-up and top-down. Common seasonal patterns in

*Tel.: +43-6232-312534; fax: +43-6232-3578.

E-mail address: katrin.teubner@assoc.oew.ac.at,
Katrin.Teubner@oew.ac.at (K. Teubner).

phytoplankton communities of deep stratifying lakes are summarised e.g. in Reynolds [2].

With a maximum depth of 190 m and a water volume of $2302 \times 10^6 \text{ m}^3$ Traunsee, is the deepest alpine lake in Austria. Industrial salt and alkaline sludge have been deposited in the Ebensee bay (EB) since 1883. I studied the impact of these tailings on phytoplankton by comparing the seasonal and the vertical patterns of algae and nutrient resources between the impacted in-shore site EB and an open water reference station (VI) in Traunsee. In particular, correlative relationships were used to search for a significant distinct species composition, algal community size structure and absolute concentration of the main nutrient elements.

In freshwater systems phosphorus is usually the major bottom-up element controlling productivity. Beside the concentration of P, the proportion between P-fractions and the relationship between P and other nutrients [3] are key factors for the relative availability of resources for algal growth and plankton community. Portions between the fractions within total phosphorus (TP) as described by the triple ratio DRP:DOP:PP reflect biomass, the P-availability for producers (e.g. [4]) and the P-release by producers and consumers. A second triple ratio, N:P:Si concerns the stoichiometric relationship between nutrients in planktonic matter. We used the molar ratio TN:TP:SRSi = 16:1:17 as a reference point for the ecological stoichiometry of shallow meso- to hypertrophic lakes, and could show that, commonly TN or TP or SRSi is invariant relative to the remaining other two elements ([3]; TN = total nitrogen, SRSi = soluble reactive silica). Lakes where TN:TP:SRSi fluctuated evenly around this reference point, in a cyclic pattern throughout the seasons, were the exception to the rule.

I hypothesise that significant differences between the impacted in-shore site and the open water reference site in oligotrophic Traunsee become evident by the pattern of both (i) the seasonal structure and (ii) the vertical distribution of phytoplankton and nutrients. Further I focus on the use of P-sources by the share of fractions within TP and the stoichiometry of N:P:Si.

2. Methods

Monthly measurements in Traunsee were recorded at a station close to the industrial outlet in the EB and the reference site at the maximum depth of 190 m near Viechttau (VI) from December 1997 to October 1998.

TN, dissolved inorganic N ($\text{DIN} = \text{NO}_3^- - \text{N} + \text{NO}_2^- - \text{N} + \text{NH}_4^+ - \text{N}$), SRSi, the fractions of TP as dissolved reactive P (DRP), total dissolved P (DP), dissolved non-reactive P (DOP), dissolved non-reactive P ($\text{DOP} = \text{DP} - \text{DRP}$, mainly dissolved organic P), particulate P ($\text{PP} = \text{TP} - \text{DP}$ [5]) and chlorophyll-*a* (Chl-*a*) were mea-

sured from discrete samples at different depths using standard techniques.

All other abbreviations, descriptions, methods and units for variables are summarised in Table 1.

Logarithmic data were standardised for multivariate statistical analyses using STATGRAPHICS plus 4.0 and SYSTAT 8.0. A step-wise species extraction was repeated with principal component analysis (PCA) until the first two components represented more than 50% of total variance (13 taxa in Fig. 3A, 22 cases). Those species extracted by PCA were included in the discriminant analysis (DA, Fig. 3B).

Triple ratios of the three fractions as DRP:DOP:PP and of nutrient stoichiometry as N:P:Si are displayed in triangular diagrams using Grapher 1.22 (Fig. 5). Each point on the triangle represents the sum of the three P-fractions or the concentration of the three nutrients equal to 100%. The corners of the triangle represent the concentration of one element only (100%) and the absence of the remaining two. Points near the corner PP in Fig. 5A and D indicate a high proportion close to 100% within TP, those distant from the PP corner low proportions. Points on the DRP:DOP-axis would mark the absence of PP (0%). The central intersection point of the three solid lines marks the equal proportion among the three fractions ($\text{DRP:DOP:PP} = 33:33:33 = 1:1:1$). The solid line intersecting the PP-corner indicates the constant ratio of equal proportions between DRP and DOP (e.g. $\text{DRP:DOP} = 50:50$) at variable PP. In analogy the other two solid lines mark equal proportions between PP:DOP at variable DRP and DRP:PP at variable DOP, respectively.

I assume that the molar 'optimum ratio' N:P:Si = 16:1:17, which in a strict sense refers to cellular content only, reflects the stoichiometric demand by the algal organisms and is used as a reference point for ecological stoichiometry [3]. For that scaling reason the relative concentrations were calculated by $C_{\text{TN}} = C_{\text{TN orig}}/R_{\text{TN}}$, $C_{\text{TP}} = C_{\text{TP orig}}/R_{\text{TP}}$ and $C_{\text{SRSi}} = C_{\text{SRSi orig}}/R_{\text{SRSi}}$ with $R_{\text{TN}} = 16$, $R_{\text{TP}} = 1$ and $R_{\text{SRSi}} = 17$. Consequently, the three optimum lines of N:P = 16:1, N:SRSi = 16:17 and P:SRSi = 1:17 are displayed in the triangle (Fig. 5B) in the proportion 1:1 (50%:50%). The optimum ratio of N:P:SRSi = 16:1:17 is marked by the intersection of these three optimum lines. This scaling is valid for Figs. 5C and E too, but only the highlighted bold inner triangle from Fig. 5B is shown.

3. Results

The range of annual variation of TP, the portion of P which was accumulated by organisms (%PP of TP) and the chlorophyll-*a* (chl-*a*) for the depths 5 and 10 m is displayed as notched box whisker plots for the open water reference site (VI) and the impacted site (EB) in

Table 1
Abbreviations, descriptions and units for variables

Abbr.	Description	Unit
Phyt biovol	Phytoplankton biovolume; light microscopy counts and size measurements, mean values of single species of a normal or a log-normal distribution were calculated depending on the best fit.	$\text{mm}^3 \text{l}^{-1}$
S	Phytoplankton surface same as above	$\text{mm}^2 \text{l}^{-1}$
S:V	Surface: (bio)volume ratio of phytoplankton	$\text{mm}^2 \text{l}^{-1}; \text{mm}^3 \text{l}^{-1}$
C _p	Carbon of phytoplankton; calculated separately for classes, Behrendt [6]: 9.43 ng C μg^{-1} FW for cyanobacteria, 7.26 ng C μg^{-1} FW for diatoms, 6.73 μg C μg^{-1} FW for other eukaryotic algae	$\mu\text{mol}(\text{C})\text{l}^{-1}$
C _b	Carbon of heterotrophic bacterioplankton; bacterial abundance and biovolume measured by DAPI staining epifluorescence microscopy [7]; carbon calculated by volume ^{0.72} , Norland (1993) in Klammer et al. [7]	$\mu\text{mol}(\text{C})\text{l}^{-1}$
C _p :C _b	Carbon ratio of phytoplankton to bacterioplankton	$\mu\text{mol}(\text{C})\text{l}^{-1}; \mu\text{mol}(\text{C})\text{l}^{-1}$
C _{Cil}	Carbon of ciliates; abundance and biovolume of ciliates measured by quantitative Protargol staining, Sonntag et al. [9]; carbon calculated by volume conversion factor: 0.19 pg C μm^{-3} , Putt and Stoecker [8]	$\mu\text{mol}(\text{C})\text{l}^{-1}$
HNFs	Heterotrophic nanoflagellates; counting by DAPI staining, epifluorescence microscopy, Sonntag et al. [9]	$\mu\text{m}^3 \text{l}^{-1}$
C _{HNF}	Carbon of HNFs calculated by volume conversion factor: 220 fg C μm^{-3} , Sonntag et al. [10]	$\mu\text{mol}(\text{C})\text{l}^{-1}$
C _{MZOO}	Carbon of metazoan zooplankton; abundance and biovolume of rotifers, cladocerans and copepods by light microscopy; carbon by volume conversion factor: 7.87 ng C μg^{-1} FW, Behrendt [6]	$\mu\text{mol}(\text{C})\text{l}^{-1}$
C _{Cil+HNF} :C _{MZOO}	Carbon ratio of ciliates and HNFs versus metazoan zooplankton	$\mu\text{mol}(\text{C})\text{l}^{-1}$
C _z	Zooplankton carbon as the sum of carbon content of HNFs, ciliates and metazoan zooplankton	$\mu\text{mol}(\text{C})\text{l}^{-1}$
C _z :C _{b+p}	Ratio of carbon of zooplankton to pooled carbon of bacteria and phytoplankton	$\mu\text{mol}(\text{C})\text{l}^{-1}; \mu\text{mol}(\text{C})\text{l}^{-1}$
Z _{eu}	Euphotic depth; depth of 1% light intensity calculated from vertical attenuation coefficient by individual underwater light profiles (PAR, Li-COR, 4 π)	m
Z _{mix}	Mixing depth; calculated from the depth with maximum relative thermal resistance against mixing (RTR), temperature measured by the multi-parameter profile YSI 6920.	m
NTU	Nephelometric turbidity units; measured by the multi-parameter profiler YSI 6920.	

Fig. 1. The surface layers 5 and 10 m are representative for the euphotic layer at both sites in Traunsee as indicated by the mean euphotic depth of 12 and 10 m at VI and EB, respectively measured by vertical light attenuation.

TP is evidently higher at EB than at VI even if the difference is not significant as indicated by medians at the notches. Slightly lower values are found for %PP of TP and Chl-*a* at EB (median: 11% less P-accumulation and 14% less Chl-*a* than at VI). The

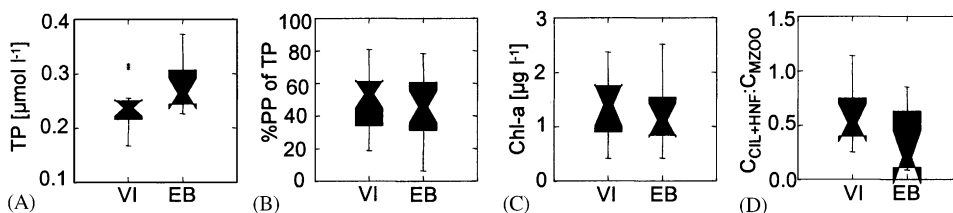


Fig. 1. (A–D) Notched box whisker plots for the significance of differences between VI and EB from 1997 to 1998, (A–C) TP, %PP of TP and chlorophyll-*a* (*chl-a*) for surface depth (5–10 m), (D): carbon ratio of ciliates and HNFs versus metazoan zooplankton inclusive rotifers ($C_{\text{Cil+HNF}}:C_{\text{MZOO}}$) as integral for the total water column at VI (0–180 m) and EB (0–40 m). Boxes are notched at the median, the length of the notches indicate 95% confidence intervals.

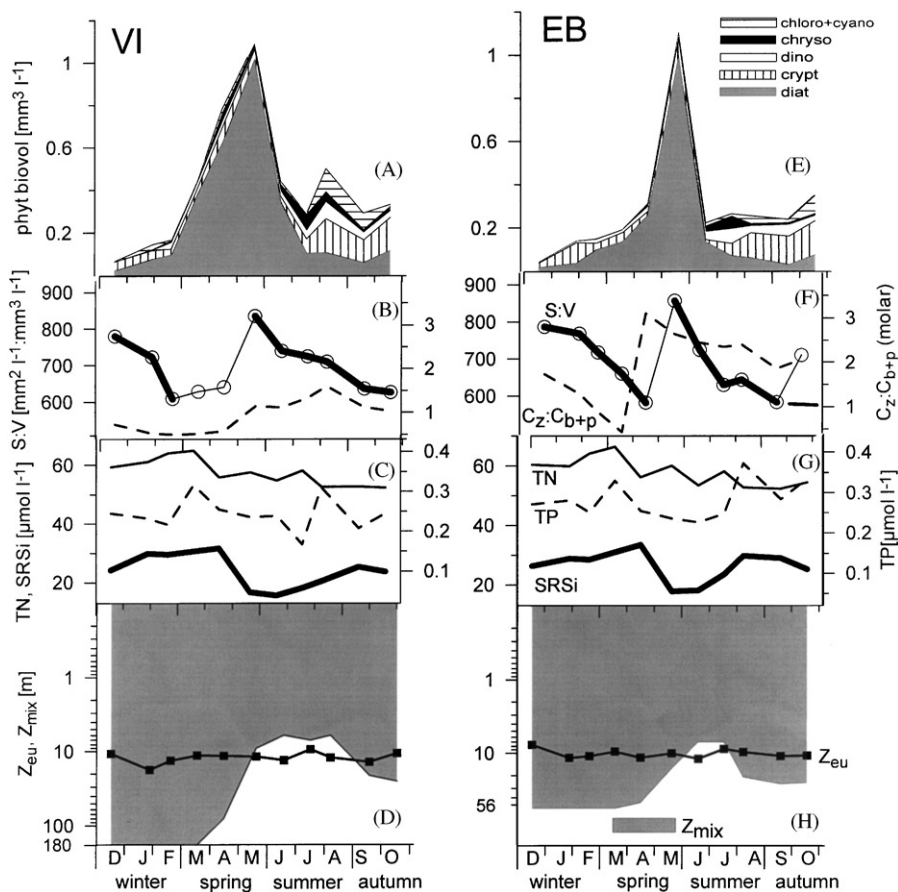


Fig. 2. (A–H) Seasonal dynamic of phytoplankton biovolume, nutrients and physical properties at VI (A–D) and EB (E–H). A, E: Algae at 10 m; legend from top to bottom: chlorophytes plus cyanobacteria, chrysophytes, dinoflagellates, cryptophytes, diatoms. B, F: S:V ratio of phytoplankton at 10 m and the ratio of zooplankton carbon: pooled carbon of bacterio- and phytoplankton ($C_z:C_{b+p}$, ratio of areal concentrations for water column 0–180 and 0–40 m, respectively; $\text{mmol m}^{-2}:\text{mmol m}^{-2}$). C, G. TN, TP and SRSi at 10 m. D, H: Euphotic depth (z_{eu}) and mixing depth (z_{mix}), notice the logarithmic scale. Zooplankton as in Fig. 1.

higher concentrations of TP at the impacted site EB are therefore neither associated with an enhanced proportion of P utilised by organisms nor, in particular, by higher algal biomass. Seasonal patterns (Figs. 2 and 3) and vertical distributions (Figs. 4 and 5) of this discrepancy are outlined now.

The seasonal dynamics of phytoplankton, nutrients, mixing and euphotic depths for VI and EB are shown in Fig. 2A–H. Phytoplankton exhibited a similar seasonal pattern at both sites (Fig. 2A and E). The annual biovolume maximum of $1.1 \text{ mm}^3 \text{ l}^{-1}$ at both sites was reached in May immediately before the onset of thermal

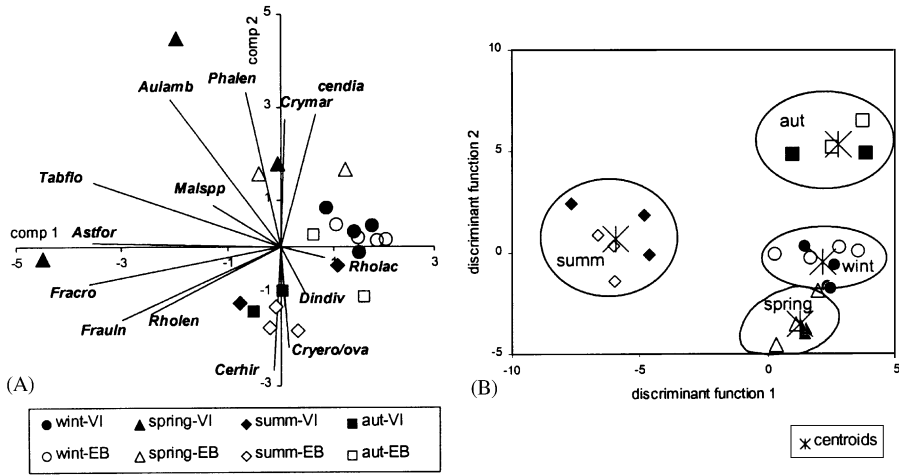


Fig. 3. Seasonal pattern of phytoplankton for VI and EB: (A) PCA: biplot of the second vs. the first component. Abbr. of algae: *Astfor*-*Asterionella formosa*, *Aulamb*-*Aulacoseira ambigua*, *Cryero/ova*-*Cryptomonas erosalovata*, *Crymar*-*C. marssonii*, *Cerhir*-*Ceratium hirundinella*, *Dindiv*-*Dinobryon divergens*, *Rholac*-*Rhodomonas lacustris*, *Rholen*-*R. lens*, *Tabflo*-*Tabellaria flocculosa*, *Fracro*-*Fragilaria crotonensis*, *Frauln*-*F. ulna*, *Phalen*-*Phacotus lenticularis*, *Malspp*-*Mallomonas* spp., *cendia*-centric diatoms, point labels: wint-winter, spring, summ-summer, aut-autumn for VI and EB, respectively, variance for components: 30% + 25% = 55%. (B) DA: plot of the second vs. the first function; algae, symbols and seasons as in A, variance for functions: 56% + 37% = 93%, overall success rate of correctly classified seasons = 96% of cases.

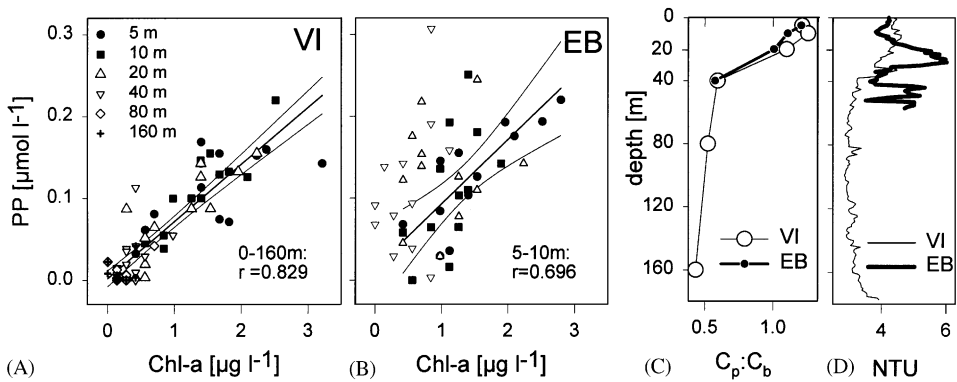


Fig. 4. (A–C) PP vs. chlorophyll-*a* (chl-*a*) for depth layers (A–B) and annual averaged carbon ratio of phytoplankton to bacterioplankton ($C_p:C_b$, C) and turbidity units (NTU, D) in depth profiles at VI and EB (coefficients from Pearson product moment correlation in A–B).

stratification (Fig. 2A–F). Diatoms contributed with 90–93% most to the phytoplankton biovolume in spring. Cryptophytes contributed 30–55% to total biovolume in late summer and autumn at both sites. Diatoms contributed on average 54% at VI and 48% at EB to total biovolume. Other algal groups such as dinoflagellates, chrysophytes, chlorophytes and cyanobacteria were of minor importance and reached not more than 26% of the total biovolume during the annual cycle. No statistically different temporal pattern between VI and EB could be found for any algal group ($p > 0.05$, *t*-test).

The relationship between the total-surface and the total-volume of phytoplankton was used as a measure

for the size structure within the algal community. This surface:volume ratio (S:V) showed a similar seasonal trend for both sites (Fig. 2B–F, $p > 0.05$, *t*-test). High S:V ratios were observed in December–January and in May indicating the relative dominance of algae with a relative high cell surface but low cell volume. The winter peak is mainly due to dominance of small cryptophytes, e.g. *Cryptomonas pusilla*, *Rhodomonas lacustris* and small unicellular centric diatoms. The spring peak referred to higher abundance of unicellular centric diatoms and needle-shaped pennate diatoms, e.g. *Fragilaria ulna* and *Asterionella formosa*. The S:V ratio (Fig. 2B and F) is inversely related to concentrations of

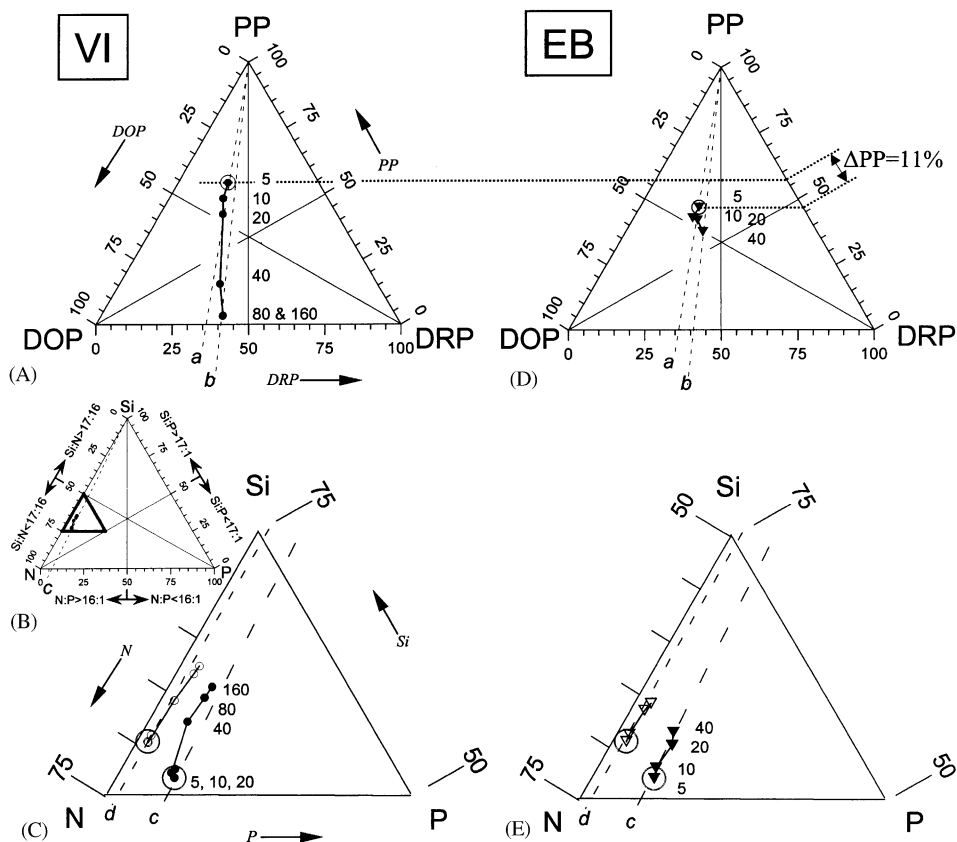


Fig. 5. (A–E) Proportion between fractions of TP as DRP:DOP:PP and the stoichiometry of N:P:Si for depth profiles at VI (A–C) and EB (D–E). Annual averages for depths were indicated by numbers: VI-5, 10, 20, 40, 80 and 160 m, EB-5, 10, 20 and 40 m; upper surface (5 m) marked by an open circle. The central intersection point of the three solid lines indicates the proportion of DRP:DOP:PP = 1:1:1 (A, D) and N:P:Si = 16:1:17 (B) see method. The bold triangle in B is displayed in C and E. The open symbols in C and E show the proportion between inorganic dissolved fractions as DIN:SRP:SRSi, the filled symbols the ratio between total N, total P and SRSi (TN:TP:SRSi). Lines a–b and arrows in A are valid for A and D, $\Delta PP = 11\%$ in D is the difference of %PP between VI and EB, lines c–d and arrows in C for C, D and E, explanation see text.

SRSi (Fig. 2C and G) in the photic zone at both sites (VI: $r = -0.66$, $p = 0.03$; EB: $r = -0.61$, $p = 0.04$). A weaker non-significant correlation is found to Si:TP (VI: $r = -0.57$, EB: $r = -0.46$), but no correlation was observed between S:V and the carbon ratio of the zooplankton to the pool of bacterio- and phytoplankton integrated over the total water column ($C_z:C_{b+p}$ in Fig. 2B and F).

The seasonal dynamics of TN, TP and SRSi were almost identical at both sites (Fig. 2C and G). SRSi and TP were low during the spring peak of algae and thermal stratification (Fig. 2D and H). The water column was stratified from May to September at VI but only for a short period from June to July at EB. The euphotic depth therefore exceeded the mixing depth 2 months longer in VI than in EB. Between-site optical properties (vertical attenuation, euphotic depth) are statistically significant (paired t -test, $p < 0.05$). The euphotic depth was on average 2 m higher at the open water reference

site VI than at EB. The other parameters of the euphotic layer described above, however, were statistically not different between sites (paired t -test, $p > 0.05$).

PCA and DA illustrate the phytoplankton structure at 10 m for VI and EB (Fig. 3A and B). According to these analyses the representative algae were *Mallomonas* spp., *Rhodomonas lacustris*, unicellular centric diatoms and *Asterionella formosa* for winter; *Fragilaria ulna*, *F. crotonensis*, *Cryptomonas marssonii* and unicellular centric diatoms for spring; *Phacotus lenticularis*, *Ceratium hirundinella*, *Cryptomonas marssonii*, *Rhodomonas lens*, *Fragilaria ulna* and *Dinobryon divergens* for summer and *Mallomonas* spp., *Dinobryon divergens*, *Cryptomonas ovata/erosa*, *Rhodomonas lacustris*, *R. lens* and *Asterionella formosa* for autumn. Points for PCA and DA were labelled according to seasons and sites. PCA shows that points of the same season of VI and of EB are clustered together indicating the similarity of the seasonal composition at both sites (Fig. 3A). The result

Pages 1589-1590 not shown

K. Teubner / Water Research 37 (2003) 1583–1592

recycled at longer intervals from the organic matter, P and N are rapidly recycled, thus, particulate Si supports much less or nothing at all to the regenerated production than the respective fraction of P or N (e.g. [14,15]), (ii) species of phytoplankton have no storage capacity for Si, but can store P and N intracellularly (e.g. polyphosphate bodies, cyanophycin granules in cyanobacteria) which can be utilised for growth after external inorganic dissolved N and P is exhausted. Consideration of only inorganic dissolved N and P would ignore the potential growth by stored resources. Thus TN and TP are better estimators of the nutrient pool utilised for algal growth than their respective dissolved fractions (cf. [2,16]). This opinion is also supported by the fact that no between-site difference for DIN:DRP:SRSi exists in Traunsee. Not surprisingly, profiles of DIN:DRP:SRSi at both sites reflect mainly the same the general vertical pattern of the decrease of DRP and SRSi with depth.

Because P is the most severe limiting nutrient element in the oligotrophic Traunsee, the question arises how efficiently P is utilised, recycled and accumulated by planktonic organisms. P evaluated along a depth profile by both the DRP:DOP:PP and the TN:TP:SRSi ratio show, that the epilimnetic plankton community at the open reference site VI retains relatively more P in the cells (PP) or as total concentration (TP) than at the impacted site EB. The enhancement of %PP of TP implies indirectly a more efficient uptake or less losses due to (i) higher affinity to all dissolved P-fractions by bacteria and algae (e.g. [4]), (ii) higher storage capacity in algae and (iii) recycling at shorter turnover time (e.g. [17]; more on zooplankton see below). The epilimnetic P shift towards TP but not towards DRP relative to the other nutrients support again the adaptation of the plankton community to the most limiting element in the epilimnion, especially when considering that the absolute pool size of TP is lower at VI than at EB (Fig. 1A).

Si indicates best the layers of algal growth, because it is the only nutrient in the triple ratio which is utilised by algae only and therefore much less involved in regenerated production than N or P. Si is important for new production in stratified lakes after replenishment by mixing, eddy diffusion from deeper water into the euphotic zone and external load (e.g. [14,15]). The layer of phytoplankton activity, therefore, is highlighted by Si-exhaustion relative to N and P. Accumulation processes dominate over decomposition processes at this layer of phytoplankton dominance and result in accumulation and stoichiometric shifts toward P. Similar observations were made when P-reduction shifted a lake from eutrophic to mesotrophic in Alte Donau [18]. The accumulation of that element which is limiting is a common phenomenon as e.g. shown by data from Behrendt [6] when re-evaluated by triple ratios of C:N:P. In lake Müggelsee P-rich algal cells dominate at periods of P-limitation (diatoms and other eukaryotic

species during spring and autumn [6]), while N-rich algae (cyanobacteria during summer [6]) at N-limitation [3].

According to the $C_p:C_b$ ratio of 1.2 the contribution of the bacterial carbon is almost the same as the algal carbon in the euphotic layer of oligotrophic Traunsee. This ratio is in the range of other studies and confirms the common phenomenon of increased significance of bacteria relative to algae with decreased standing crop of algae or productivity (e.g. [20]).

Zooplankton composition is assumed to be an important component of the plankton community at VI affecting the relative increase of PP at lower TP concentrations. Nutrient cycling by ciliates and HNFs is more important at VI than at EB as can be assumed from the higher carbon ratio of microzooplankton to metazoan-zooplankton at VI. In contrast to this 'microbial loop', cycling by the 'classical food chain' is more relevant for EB (Figs. 1D, 2B and F). It has been accepted that energy and nutrients are most efficiently transferred from lower to higher trophic levels via 'microbial loop'. Nutrient regeneration by micro-zooplankton therefore becomes more important as the overall productivity decreases in an increasingly resource-limited lake [20].

The differences between sites are expressed by different forms of the average vertical profiles of DRP:DOP:PP and TN:TP:SRSi. Reasons for the disturbance at the impacted by less P-accumulation of organisms in euphotic layer and a spatially reduced trophogenic zone to the top 10m marked by Si exhaustion relative to TN and TP are: unstable stratification due to the input of industrial tailings at 2 and 20 m, a turbidity plume at 20–40 m, the enlarged size of TP by industrial effluents and the metazoan dominated food chain. The area of the EB at the impacted site is about 0.3 km², corresponding to only 1.2% of the total area of the lake. Because of the strongly localised disturbance near the impacted site, the effects on the plankton community are insignificant for the lake in total.

5. Conclusions

1. Annual averages of ratios for the proportion between P-fractions and for stoichiometry between P and other nutrients (DRP:DOP:PP and TN:TP:SRSi) are sensitive indicators to identify TP pool-size related effects and the distribution of phytoplankton along depth gradients in deep oligotrophic lakes.
2. Significant differences between the open-water reference site and the impacted site are evident from vertical profiles of both the P-accumulation (%PP of TP) evaluated by DRP:DOP:PP and the distribution of phytoplankton assessed by Si-exhaustion

- (TN:TP:SRSi), but not from the seasonal patterns of phytoplankton composition, S:V ratios of the algal community or surface layer nutrient dynamics.
- As indicated by depth profiles of DRP:DOP:PP and TN:TP:SRSi the disturbances due to unstable stratification and higher turbidity at the impacted site are: (i) up to 11% less P-accumulation by organisms at the surface, (ii) no stoichiometric shift towards TP in the euphotic layer when compared with deeper layers and (iii) a spatially reduced trophogenic zone to the top 10 m marked by Si exhaustion in coincidence with the layer of the pre-dominance of the phytoplankton versus the bacterioplankton.
 - Site VI represents the undisturbed open-water oligotrophic situation in lakes. Both the higher portion of particulate P within TP and the shift towards P-enrichment in nutrient stoichiometry of TN:TP:SRSi verify the relative P-accumulation in the euphotic depth by planktonic community in the open water of deep oligotrophic lakes.

Acknowledgements

I am very grateful to C. Skolaut and H. Gollmann for help with sampling and chemical analyses, to B. Sonntag, S. Klammer, T. Posch and C. Jersabek for making basic data of bacteria, HNFs and zooplankton available. I thank M.T. Dokulil and R. Psenner for improving an earlier draft of the manuscript, the two anonymous reviewers for constructive criticism and Stephen Lowry for improving the English. The investigations were funded by the Government of Upper Austria.

References

- Lewis Jr. WM. Surface/volume ratio: implications for phytoplankton morphology. *Science* 1976;192:885–7.
- Reynolds CS. *Vegetation processes in the pelagic: a model for ecosystem theory*. Oldendorf: Ecology Institute, 1997.
- Teubner K, Dokulil MT. Ecological stoichiometry of TN:TP:SRSi in freshwaters: nutrient ratios and seasonal shifts in phytoplankton assemblages. *Arch Hydrobiol* 2002;154:625–46.
- Coveney MF, Wetzel RG. Biomass, production and specific growth rate of bacterioplankton and coupling to phytoplankton in an oligotrophic lake. *Limnol. Oceanogr* 1995;40:1187–200.
- Psenner R, Pucsko R. Phosphorus fractionation: advantages and limits of the method for the study of sediment P origins and interactions. *Arch Hydrobiol Beih Ergebn Limnol* 1988;30:43–59.
- Behrendt H. The chemical composition of phytoplankton and zooplankton in a shallow lake. *Arch Hydrobiol* 1990;118:129–45.
- Klammer S, Posch T, Sonntag B, Griebler C, Mindl B, Psenner R. Dynamics of bacterial abundance, biomass, activity, and community composition in the oligotrophic Traunsee and the Traun River (Austria). *Water Air Soil Pollut Focus* 2002;2:137–63.
- Putt M, Stoecker DK. An experimentally determined carbon: volume ratio for marine oligotrichous ciliates from estuarine and coastal waters. *Limnol Oceanogr* 1989;34:1097–103.
- Sonntag B, Posch T, Psenner R. Comparison of three methods for determining flagellate abundance, cell size, and biovolume in cultures and natural freshwater samples. *Arch Hydrobiol* 2000;149:337–51.
- Sonntag B, Posch T, Klammer S, Griebler C, Psenner R. Protozooplankton in the deep oligotrophic traunsee (Austria) influenced by discharges of soda and salt industries. *Water Air Soil Pollut Focus* 2002;2:211–26.
- Smith REH, Kalff J. Competition for phosphorus among co-occurring freshwater phytoplankton. *Limnol Oceanogr* 1983;28:448–64.
- Teubner K, Sarobe Egiguren A, Vadrucci MR, Dokulil MT. ¹⁴C Photosynthesis and pigment pattern of phytoplankton as size related adaptation strategies to the underwater light gradient in alpine lakes. *Aquat Sci* 2001;63:310–25.
- Grover JP. Influence of cell shape and size on algal competitive ability. *J Phycol* 1989;25:402–5.
- Caraco NF, Cole JJ, Likens GE. New and recycled primary production in an oligotrophic lake: insights for summer phosphorus dynamics. *Limnol Oceanogr* 1992;37:590–602.
- Dugdale RC, Minas HJ. The role of the silicate pump in driving new production. *Deep-Sea Res* 1995;42:697–719.
- Sommer U. A comment on the proper use of nutrient ratios in microalgal ecology. *Arch Hydrobiol* 1999;146:55–64.
- Queimaliños CP, Modenutti BE, Balseiro EG. Phytoplankton responses to experimental enhancement of grazing pressure and nutrient recycling in a small Andean lake. *Freshwater Biol* 1998;40:41–9.
- Teubner K, Donabaum K, Kabas W, Kirschner A, Pfister G, Salbrechter M, Dokulil MT. Enhanced phosphorus accumulation efficiency by the pelagic community at reduced phosphorus supply: a lake experiment from bacteria to metazoan zooplankton 2002; in press.
- Teubner K, Dokulil MT. ¹⁴C-photosynthesis of phytoplankton in an oligotrophic alpine lake and its response to turbidity by industrial tailings (Traunsee, Austria). *Water Air Soil Pollut Focus* 2002;2:181–90.
- Capblancq J. Nutrient dynamics and pelagic food web interactions in oligotrophic and eutrophic environments— an overview. *Hydrobiologia* 1990;207:1–14.